Command Shaping Under Nonsymmetrical Acceleration and Braking Dynamics

Thomas H. Bradley

Jon Danielson

Jason Lawrence

William Singhose

Georgia Institute of Technology,
Atlanta, GA 30332-0405

The conventional unity magnitude zero vibration (UM-ZV) command shaping technique is an effective means for eliminating vibration in linear mechanical systems with on-off actuators. This paper discusses how the UM-ZV command shaping technique is affected by a common nonlinearity: nonsymmetrical accelerating and braking dynamics. Two approaches for creating new types of UM-ZV shaped commands are presented: a closed-form analytic solution and a numerical optimization approach. Both methods reduce residual vibration of the nonlinear system more effectively than the conventional UM-ZV shaped commands. Simulations and experiments on a bridge crane confirm the effectiveness of the new commands. [DOI: 10.1115/1.2948385]

1 Introduction

Many mechanical systems accelerate at a different rate than they decelerate. This effect can be due to separate actuation mechanisms, noncolocated actuators, or unilaterally dispersive dynamics. For example, nonsymmetrical acceleration-braking is a common nonlinearity associated with overhead cranes. This nonlinearity is present in cranes which use a torque-limited electric motor to accelerate the crane trolley and a friction brake to decelerate the crane trolley. This causes the crane trolley to accelerate at a different rate than it decelerates, complicating position control and oscillation suppression.

Input shaping has been proposed as a means to reduce the vibration of oscillatory systems [1–4]. The input shaping process is open loop, requires no extra sensors, and is easy to implement, but is most effective for linear systems. For nonlinear systems, modifications to conventional input shaping techniques must be made to account for the nonlinearity [5–8]. The goal of this research effort is to develop input shaping techniques that are effective for the nonsymmetrical acceleration-braking nonlinearity. The results of this study are applicable to a wide variety of systems whose nonlinearities can be modeled using the nonsymmetrical acceleration-braking framework.

This article proposes a generalized model of the nonlinear dynamics of such a system and describes the detrimental effect of the nonsymmetrical acceleration-braking nonlinearity on conventional unity magnitude zero vibration (UM-ZV) input shapers [9]. Next, the derivation of a UM-ZV input-shaped command that can effectively cancel the oscillation of this nonlinear system under a limited range of parameters is presented. Finally, a numerical optimization technique is used to derive a UM-ZV shaped command that can be applied to a much wider range of parameters. Comparisons of the effectiveness of all three UM-ZV shaped commands are made through simulation and experiments.

Contributed by the Technical Committee on Vibration and Sound of ASME for publication in the JOURNAL OF VIBRATION AND ACOUSTICS. Manuscript received February 19, 2007; final manuscript received February 26, 2008; published online August 13, 2008. Assoc. Editor: Christopher D. Rahn. Paper presented at the 2006 ASME International Mechanical Engineering Congress (IMECE2006), Chicago, IL, Nov. 5–10, 2006.

2 Background

An input shaper is a series of impulses that have a zero in frequency domain at a design frequency ω. To form an input-shaped command, the series of impulses is convolved with any desired baseline command. The convolution process preserves the frequency domain properties of the input shaper, and the input-shaped command will contain zero energy at the design frequency. Linear systems actuated by the input-shaped command will not exhibit oscillation at the design frequency.

The UM-ZV input shaper is chosen as the focus of this research effort because it can be used to form faster commands than other input shapers. Also, the UM-ZV commands can be implemented using on/off actuators, such as the "constant speed" AC motors common in small industrial cranes. A velocity pulse of the crane trolley will be used as the baseline command for this investigation. A UM-ZV shaped velocity pulse with a design frequency of $\omega=2\pi/T$ is shown in Fig. 1.

A block diagram showing the command signals, actuators, and a planar crane is shown in Fig. 2. The unshaped command, $r(t)$, is a pulse of duration t_p. This signal passes through an input shaper to form the shaped command, $r_s(t)$. The shaped command is sent to the nonlinear actuation block that outputs the actual trolley velocity, $v(t)$. For this investigation, the nonsymmetrical acceleration-braking nonlinearity is modeled as differing acceleration and deceleration first-order time constants. The actual velocity will accelerate to the commanded speed with an exponential rise characterized by a time constant, τ_a, and decelerate with a different time constant, τ_b. The crane block determines the payload response, $y(t)$, to the trolley velocity, $v(t)$, using the equation of motion of the payload: $\ddot{y}(t)+(g/L)y=-\dot{v}(t)$. This formula assumes a small vibration amplitude and a constant payload suspension length, L.

The controller architecture shown in Fig. 2 was implemented both in simulation using MATLAB™ SIMULINK™ and experimentally using an instrumented bridge crane. The instrumented crane has a $1\times1\times1$ m^3 workspace and is actuated by Siemens motors, drives, and a programmable logic controller (PLC). The suspended payload deflection is recorded with a digital camera. The maximum velocity of the crane trolley, $v_{\max}$, is 0.17 m s^{-1} and the nominal payload suspension length, L, is 0.84 m.

The output of both the simulated and experimental systems is the payload displacement $y(t)$ as a function of the parameters of the input-shaped command (t_1, t_2, t_3, t_4, t_5, $v_{\max}$, t_p), the parameters of the payload (L), and the parameters of the actuation nonlinearity (τ_a, τ_b). The parameters of the payload, unshaped pulse ($v_{\max}$, t_p), and actuation nonlinearity will be given for any problem. The goal is to determine the parameters of the input-shaped command so as to minimize residual vibration.

3 UM-ZV Shaping With an Acceleration-Braking Nonlinearity

For a UM-ZV shaped system without any nonlinearities, the residual vibration will be zero. In the presence of the nonsymmetrical acceleration-braking nonlinearity, the performance of UM-ZV shaped commands is degraded. Figure 3 shows the magnitude of the residual vibration, as a function of the braking time constant τ_b and the velocity command pulse duration t_p, with the acceleration time constant set to $\tau_a=0.117$ s. For most of the tested conditions, there exists a significant residual vibration when using the UM-ZV input shaper to actuate the nonlinear system. The experimental results validate the results from simulation. At all points in the test matrix, the difference between the simulation

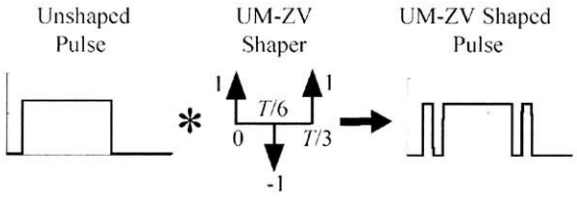

Fig. 1 UM-ZV shaper and UM-ZV shaped pulse

and the experiment is <23 mm, which is <15% of the unshaped vibration amplitude. Discrepancies between the experimental and simulated performance of the system are due to the excitation of higher-order modes in the experimental system and an imperfect model of the system nonlinearities.

It is notable that as the deceleration time constant approaches the acceleration time constant ($\tau_b \rightarrow \tau_a$=0.117 s), the magnitude of residual vibration decreases. When $\tau_b = \tau_a$, the system becomes linear, the UM-ZV commands function as designed, and the residual vibration is approximately zero. Even under the worst conditions tested, the residual vibrations from the UM-ZV command are much lower than the residual vibrations from unshaped commands. A comparison between the residual vibration for unshaped and UM-ZV shaped commands is presented in Fig. 4. In summary, the UM-ZV shaped command can significantly reduce the residual vibration of the system even when there is an acceleration-braking nonlinearity. However, the resulting system still exhibits sensitivity to the magnitudes of the acceleration and deceleration time constants and the command pulse duration. This indicates that the UM-ZV shaper cannot robustly compensate for the nonlinearity.

4 Closed-Form Compensated UM-ZV Shaping

In this section, we derive and minimize an analytical expression for the residual vibration of the UM-ZV shaped nonlinearly actuated system. This expression can be solved to find the step times $(t_1, t_2, t_3, t_4, t_5)$ of a UM-ZV shaped command that will more effectively compensate for the acceleration-braking nonlinearity.

The ramp-up portion of the trolley velocity profile can be represented as a function of the step times t_1, t_2, and t_3, as illustrated in Fig. 2, and given in this equation:

$$v(t) = \sum_i v_i(t), \quad \forall\, t > 0$$

$$\begin{aligned} v_1(t) &= v_{\max}((1 - e^{-t/\tau_a})\delta(t - t_1)) \\ v_2(t) &= -v_{\max}((1 - e^{-t/\tau_b})\delta(t - t_2)) \\ v_3(t) &= v_{\max}((1 - e^{-t/\tau_a})\delta(t - t_3)) \end{aligned} \tag{1}$$

Each term consists of a first-order response to a step command convolved with a time delayed impulse.

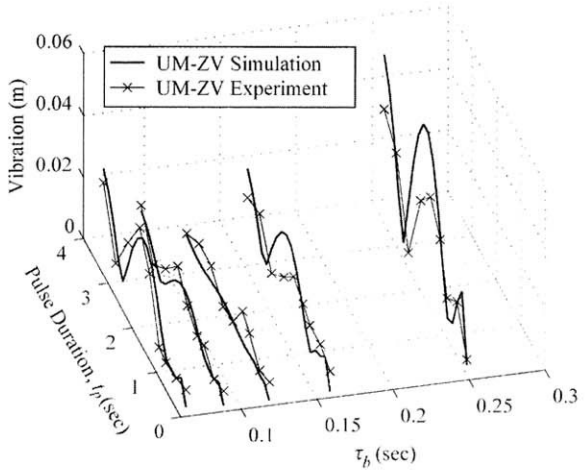

Fig. 3 Payload residual vibration using UM-ZV commands as a function of t_p and τ_b (τ_a=0.117 s)

The steady state response of a system to Eq. (1) can be derived from the linear system theory. For example, if $v(t)$ is used to drive an undamped system, then

$$y(t) = \sum_i y_i(t), \quad \forall\, t > 0 \tag{2}$$

where $y_i(t)$ is the deflection due to the ith term in Eq. (1) and is given by

$$\begin{aligned} y_i(t) &= \frac{1}{\omega}|G_i|\sin\left(\omega t - \omega t_i - \frac{\pi}{2} + \angle G_i\right) \\ |G_1| &= \frac{v_{\max}}{\sqrt{(\tau_a\omega)^2 + 1}}, \quad \angle G_1 = \tan^{-1}\left(\frac{1}{\tau_a\omega}\right) - \pi \\ |G_2| &= \frac{v_{\max}}{\sqrt{(\tau_b\omega)^2 + 1}}, \quad \angle G_2 = \tan^{-1}\left(\frac{1}{\tau_b\omega}\right) \\ |G_3| &= |G_1|, \quad \angle G_3 = \angle G_1 \end{aligned} \tag{3}$$

A more compact representation can be formed using phasor notation. Using phasor notation, the residual vibration amplitude $A(t_1, t_2, t_3)$ can be stated as

$$A(t_1, t_2, t_3) = \left|\sum_i \mathbf{y}_i\right| \tag{4}$$

where

$$|\mathbf{y}_i| = \frac{|G_i|}{\omega}, \quad \angle \mathbf{y}_i = -\omega t_i - \frac{\pi}{2} + \angle G_i$$

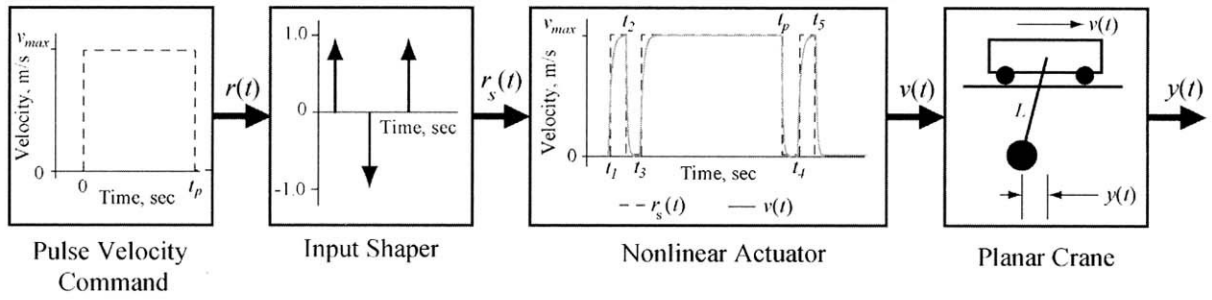

Fig. 2 Block diagram of the control and the actuation system

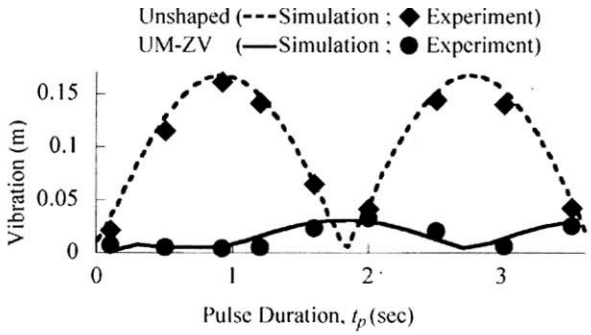

Fig. 4 Residual vibration using unshaped and UM-ZV shaped commands as a function of t_p (τ_a=0.117 s, τ_b=0.065 s)

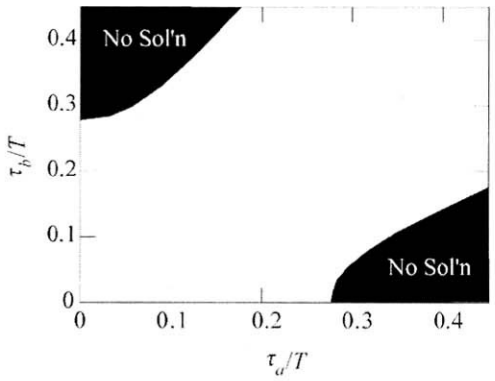

Fig. 6 Constraints on τ_a/T and τ_b/T for the UM-ZV$_c$ shaped command

To minimize the amplitude of the residual vibration, $A(t_1,t_2,t_3)$ can be set to zero. Assuming that the time of the first impulse is $t_1=0$, then

$$|\mathbf{y}_1| = 1, \quad \angle\mathbf{y}_1 = 0$$

$$|\mathbf{y}_2| = \sqrt{\frac{(\tau_a\omega)^2+1}{(\tau_b\omega)^2+1}}, \quad \angle\mathbf{y}_2 = \omega t_2 + \tan^{-1}\left(\frac{1}{\omega\tau_a}\right) - \tan^{-1}\left(\frac{1}{\omega\tau_b}\right)_i \tag{5}$$

$$|\mathbf{y}_3| = 1, \quad \angle\mathbf{y}_3 = \omega t_3$$

Two methods are available for finding the times of the second and third impulses that will yield zero residual vibration. The first method involves the substitution of Eq. (5) into Eq. (4), and the solution of the simultaneous algebraic equations for t_2 and t_3. Alternatively, a geometric approach is more efficient and insightful.

Each of the phasors in Eq. (5) can be represented as vectors, as shown in Fig. 5. When the vectors sum up to zero, they can be arranged as a triangle in the vector space and the magnitude of the residual vibration is zero. The angles of the triangle relate to the phasor angles in Eq. (5) by the relations $\angle\mathbf{y}_2=\alpha_2$ and $\angle\mathbf{y}_3=\alpha_3$. The law of cosines can be used to solve for α_2 and α_3. Substituting the results into Eq. (5) yields

$$t_2 = \frac{1}{\omega}\left(\tan^{-1}\left(\frac{1}{\omega\tau_b}\right) - \tan^{-1}\left(\frac{1}{\omega\tau_a}\right)\right) + \frac{1}{\omega}\cos^{-1}(\beta) + nT$$

$$t_3 = \frac{1}{\omega}\cos^{-1}(2\beta^2-1) + mT \tag{6}$$

$$\beta = \frac{1}{2}\sqrt{\frac{(\tau_a\omega)^2+1}{(\tau_b\omega)^2+1}}$$

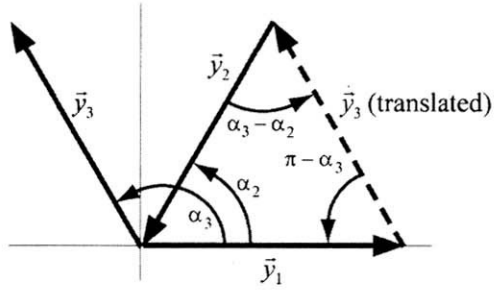

Fig. 5 Phasor diagram for UM-ZV input shaper ramp-up command

It is notable that additional solutions can be found by adding integer multiples of the system period, T, to t_2 or t_3. The non-negative integers n and m are defined such that $0 \le n \le m$, so as to ensure that $t_2 < t_3$. To solve for the ramp-down impulse times t_4 and t_5, exchange the values of τ_a and τ_b in Eq. (6) and solve for the new values of $\bar{t}_2$ and $\bar{t}_3$, where $t_4=t_p+\bar{t}_2$ and $t_5=t_p+\bar{t}_3$. This new unity magnitude shaped command is uniquely defined by the step times (t_1,t_2,t_3,t_4,t_5). In the remainder of this article it will be referred to as the UM-ZV$_c$ command.

The solution to the nonlinear acceleration-braking UM-ZV$_c$ input-shaping problem proposed in Eq. (6) is limited in its applicability. First, the acceleration or deceleration that is associated with each impulse of the UM-ZV$_c$ shaped command must be allowed to reach its final velocity before the next switch time. This is a requirement of the linear system theory employed in Eq. (2). This constraint can be approximated mathematically as

$$(t_2 > 3\tau_a) \cap (t_3 - t_2 > 3\tau_b) \cap (t_4 - t_p > 3\tau_b) \cap (t_5 - t_4 > 3\tau_a) \tag{7}$$

Meeting these constraints is accomplished simply by increasing the value of m or n in Eq. (6) until Eq. (7) is satisfied.

Second, the value of β as defined in Eq. (6) must be in the range $-1 \le \beta \le 1$ so as to ensure that $\cos^{-1}(\beta)$ is real. This provides a constraint on the values of $\omega\tau_a$ and $\omega\tau_b$ that will result in real impulse times t_2, t_3. This constraint can be physically visualized by using Fig. 5. The vibration from the acceleration impulses $(\mathbf{y}_1,\mathbf{y}_3)$ must be canceled by the vibration from the deceleration impulse $(\mathbf{y}_2)$. When $\tau_a \gg \tau_b$, then the vibration from the two acceleration steps $(\mathbf{y}_1,\mathbf{y}_3)$ is smaller than the vibration from the braking step $(\mathbf{y}_2)$ and the phasors can never sum up to zero. Mathematically, this constraint can be expressed as

$$\omega\tau_b > \frac{1}{2}\sqrt{(\omega\tau_a)^2-3}$$

$$\omega\tau_a > \frac{1}{2}\sqrt{(\omega\tau_b)^2-3} \tag{8}$$

For cases where these constraints cannot be satisfied, the analytical solution is infeasible, as shown in Fig. 6. For problems in this region of the parameter space, the numerically derived UM-ZV shaping technique proposed in the next section can provide a usable solution.

To test the effectiveness of the UM-ZV$_c$ shaped command, simulations and experiments were conducted. The residual vibration induced by the UM-ZV$_c$ command was measured for a variety of pulse times and deceleration time constants. The results are presented in Fig. 7 along with the results for the UM-ZV input-shaped commands for comparison.

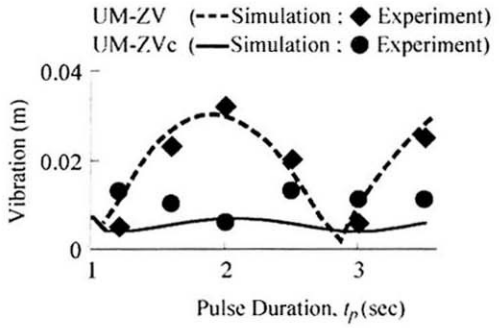

Fig. 7 Residual vibration for UM-ZV and UM-ZV$_c$ shaped commands as a function of t_p (τ_a=0.117 s, τ_b=0.065 s)

This experiment shows that the UM-ZV$_c$ shaped commands exhibit substantially improved performance over the UM-ZV shaper for the region in which they are defined. The UM-ZV$_c$ shaped commands are more robust to the acceleration-braking nonlinearity than the UM-ZV commands and produce significantly less residual vibration for most of the problem space.

5 Numerically Derived UM-ZV Shaping

The commands presented in the previous section have the advantage of being derived in a closed form. However, they are only applicable to a subset of the possible problem space, as defined by the constraints in Eqs. (7) and (8). For problems outside of these constraints, a numerical optimization method of deriving the unity magnitude shaped command is proposed. A flowchart of the design scheme is shown in Fig. 8. The impulse times for the conventional UM-ZV shaper are used to initialize the optimization routine. The MATLAB™ function fminsearch.m is used to carry out a simplex-based nonlinear optimization strategy. The optimization function calls the nonlinear system simulation at each iteration to calculate the residual vibration. The optimization cost function to be minimized is the magnitude of the payload residual vibration. When the simulated maximum residual vibration reaches a value below 0.1 mm and all constraints are satisfied, the optimization is stopped and the values of the step times (t_2,t_3,t_4,t_5) that define the optimal UM-ZV shaped command are recorded. This optimal command is labeled UM-ZV$_o$. Roughly 30 s of computation time is required to derive the UM-ZV$_o$ at a single point using MATLAB™ 6.1 on a PC with an AMD Athalon 3200 processor.

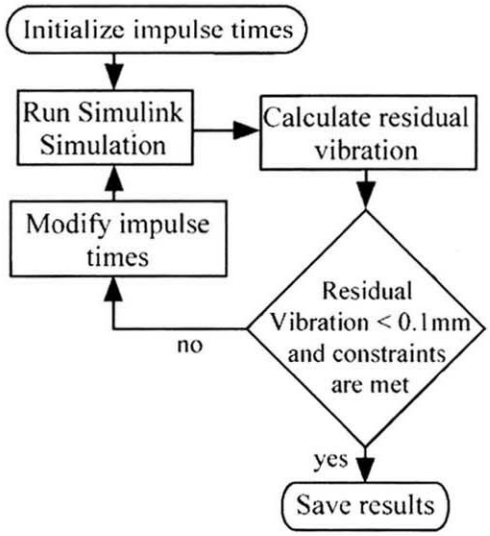

Fig. 8 Flowchart for the UM-ZV$_o$ numerical optimization routine

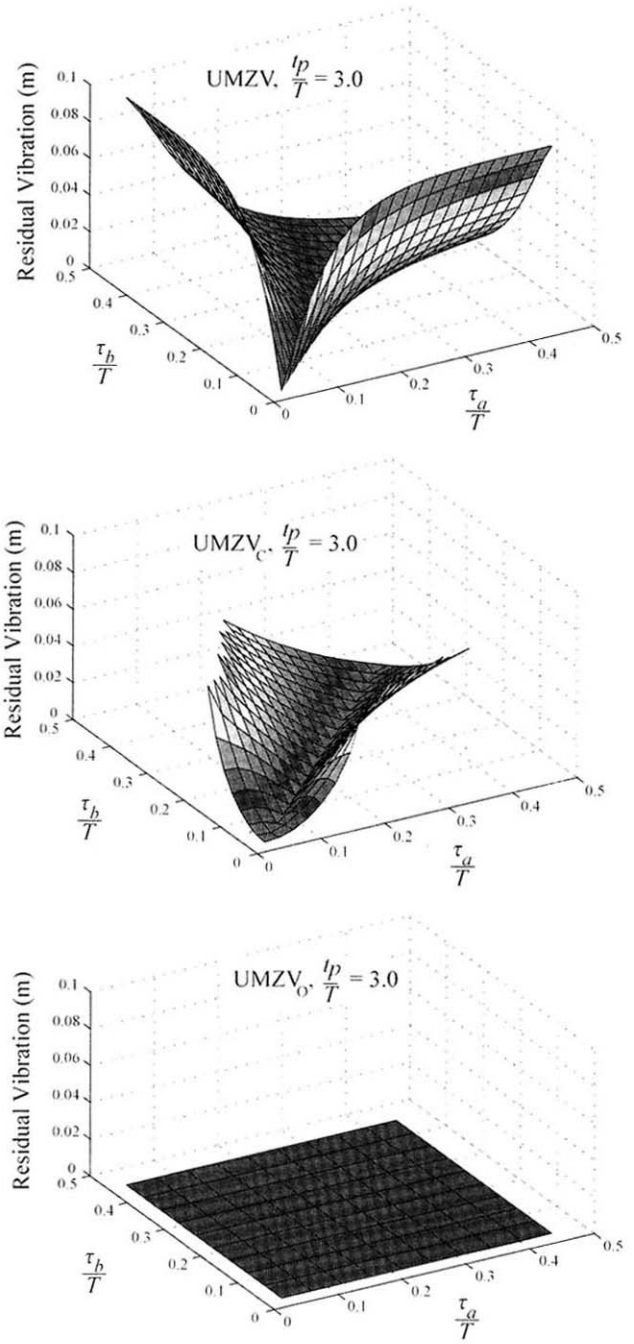

Fig. 9 Simulated residual vibration of UM-ZV shaped commands for nonlinear system

In order to determine the performance of the UM-ZV$_o$ command, this procedure was followed for 1000 evenly spaced points within the three-dimensional design space

$$\left(0.028 \le \frac{\tau_a}{T} \le 0.45\right) \cap \left(0.028 \le \frac{\tau_b}{T} \le 0.45\right) \cap \left(0.1 \le \frac{\tau_p}{T} \le 3.0\right) \tag{9}$$

The performances of the UM-ZV$_o$, UM-ZV$_c$, and UM-ZV commands in simulation are shown in Fig. 9. Each subplot shows the dependence of the system's residual vibration on τ_a/T and τ_b/T at a fixed value of τ_p/T. It is notable that along the line $\tau_a=\tau_b$, the

Table 1 Time constants and pulse widths used in experimental and numerical comparison

Experiment No.	$\frac{\tau_a}{T}$	$\frac{\tau_b}{T}$	$\frac{t_p}{T}$
1	0.187	0.123	2.03
2	0.150	0.135	1.55
3	0.113	0.147	1.06
4	0.077	0.158	0.583
5	0.040	0.170	0.100

system is linear and all three UM-ZV commands are equivalent and equally effective. In other regions of the problem space, both the UM-ZV and UM-ZV$_c$ commands show significant residual vibration. For the UM-ZV$_c$ command, the regions where the command is not defined are visible, similar to Fig. 6. In contrast, the UM-ZV$_o$ is defined and effective for the entire problem space.

A subset of the problem space, defined in Table 1, was chosen for further analysis and experimental investigation. These experiments lie along a line in the three-dimensional problem space. The residual vibration of the system was simulated continuously along the line between Experiment 1 and Experiment 5, and was experimentally measured at the five discrete points. The comparison of the effectiveness of the UM-ZV$_o$, UM-ZV$_c$ and UM-ZV commands is shown in Fig. 10.

For this comparison, the UM-ZV$_o$ command parameters (t_2, t_3, t_4, t_5) were linearly interpolated from the 1000 point dataset. This causes the response of the UM-ZV$_o$ command shown in Fig. 10 to deviate in some places from the perfect solution shown in Fig. 9.

All of the UM-ZV shaped commands outperform the unshaped commands. The UM-ZV$_c$ commands show significantly less sensitivity to the varying parameters of the nonlinearity than the UM-ZV commands. The UM-ZV$_o$ command shows the lowest residual vibration for a majority of the experiments and the highest robustness to the acceleration-braking nonlinearity.

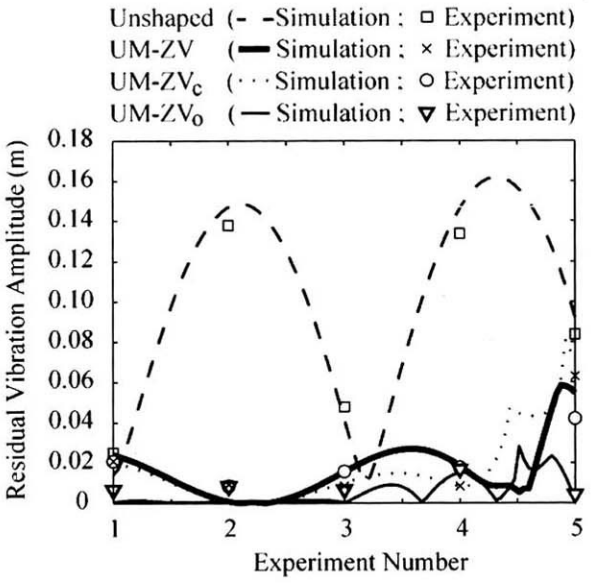

Fig. 10 Simulated and experimental responses for different UM-ZV shaped commands

6 Discussion

Despite the fact that the UM-ZV$_o$ command is more effective and robust than the other UM-ZV commands, it is not preferred in every application. Because the derivation of the UM-ZV$_o$ command is computationally costly, it is unlikely that the UM-ZV$_o$ can be derived and implemented in real time to reduce the vibration of unplanned or human operator-controlled motion. Instead, the UM-ZV$_o$ command can be calculated by interpolation from a solution dataset as was done in the experiment above. For repetitive or planned motions where the characteristics of the motion (t_p, T) are known in advance, the UM-ZV$_o$ can be derived offline and programed into the motion controller, resulting in more reliably effective UM-ZV$_o$ commands. As the UM-ZV$_c$ and UM-ZV commands are fully described by a closed-form solution, they can easily be implemented in real time or repetitive control environments.

All of the UM-ZV shaped commands derived for this study are open loop reference commands. As such, they are somewhat sensitive to errors in the model of the system. All of the shaped commands exhibit "ZV" sensitivity to errors in the model of the system's natural frequency. That is, a 10% change in natural frequency leads to an increase of approximately 15% in the ratio of shaped to unshaped residual vibration [1]. The robustness of the shaped commands to variations in acceleration and deceleration time constants is shown in Fig. 9.

7 Conclusions

The nonlinearity caused by unequal acceleration and deceleration time constants has a detrimental effect on the effectiveness of UM-ZV input shapers. Two new methods were presented to improve the performance of the UM-ZV shaped command to compensate for the nonlinearity: a closed-form solution and a numerically derived solution. The closed-form solution (UM-ZV$_c$) is more effective than the conventional UM-ZV input shaper over a limited range of problem parameters. The numerically optimized solution (UM-ZV$_o$) has improved effectiveness and a wide range of applicability, but is difficult to apply to unplanned motions. Based on the requirements of the application, a combination of any of these command shaping techniques can be used to compensate for the nonlinearity for a wide variety of problem parameters. Simulations and experimental tests demonstrated the effectiveness of the derivation techniques and resulting input-shaped commands.

References

[1] Singer, N. C., and Seering, W. P., 1990, "Preshaping Command Inputs to Reduce System Vibration," ASME J. Dyn. Syst., Meas., Control, **112**, pp. 76–82.

[2] Singhose, W., Porter, L., Kenison, M., and Kriikku, E., 2000, "Effects of Hoisting on the Input Shaping Control of Gantry Cranes," Control Eng. Pract., **8**(10), pp. 1159–1165.

[3] Agostini, M., Parker, G. G., Groom, K., Schaub, H., and Robinett, R. D., 2002, "Command Shaping and Closed Loop Control Interactions for a Ship Crane," *American Control Conference*, Anchorage, AK, pp. 2298–2304.

[4] Hong, K.-T., and Hong, K.-S., 2004, "Input Shaping and VSC of Container Cranes," *IEEE International Conference on Control Applications*, Taipei, Taiwan, pp. 1570–1575.

[5] Kinceler, R., and Peter, M., 1995, "Input Shaping for Nonlinear Systems," *American Controls Conference*, Seattle, WA, Vol. 1, pp. 914–918.

[6] Singh, T., 2004, "Jerk Limited Input Shapers," ASME J. Dyn. Syst., Meas., Control, **126**, pp. 215–219.

[7] Park, J., Chang, P. H., and Lee, E., 2002, "Can a Time Invariant Input Shaping Technique Eliminate Residual Vibrations of LTV Systems," *American Controls Conference*, Anchorage, AK, pp. 2292–2297.

[8] Lawrence, J., Singhose, W., and Hekman, K., 2005, "Friction Compensating Command Shaping for Vibration Reduction," ASME J. Vibr. Acoust., **127**, pp. 307–314.

[9] Singhose, W., Singer, N., and Seering, W., 1997, "Time-Optimal Negative Input Shapers," ASME J. Dyn. Syst., Meas., Control, **119**, pp. 198–205.